

# Development of Small-Molecule PUMA Inhibitors for Mitigating Radiation-Induced Cell Death

Gabriela Mustata<sup>1,#</sup>, Mei Li<sup>2,5,#</sup>, Nicki Zevola<sup>1#</sup>, Ahmet Bakan<sup>1</sup>, Lin Zhang<sup>3,5</sup>, Michael Epperly<sup>4,5</sup>, Joel S. Greenberger<sup>4,5</sup>, Jian Yu<sup>2,5,\*</sup> and Ivet Bahar<sup>1,\*</sup>

University of Pittsburgh School of Medicine, Departments of <sup>1</sup>Computational & Systems Biology, <sup>2</sup>Pathology, <sup>3</sup>Pharmacology and Chemical Biology, and <sup>4</sup>Radiation Oncology, and <sup>5</sup>University of Pittsburgh Cancer Institute, Hillman Cancer Center Research Pavilion, 5117 Centre Ave, Pittsburgh, PA, 15213, USA

**Abstract:** PUMA (p53 upregulated modulator of apoptosis) is a Bcl-2 homology 3 (BH3)-only Bcl-2 family member and a key mediator of apoptosis induced by a wide variety of stimuli. PUMA is particularly important in initiating radiation-induced apoptosis and damage in the gastrointestinal and hematopoietic systems. Unlike most BH3-only proteins, PUMA neutralizes all five known antiapoptotic Bcl-2 members through high affinity interactions with its BH3 domain to initiate mitochondria-dependent cell death. Using structural data on the conserved interactions of PUMA with Bcl-2-like proteins, we developed a pharmacophore model that mimics these interactions. *In silico* screening of the ZINC 8.0 database with this pharmacophore model yielded 142 compounds that could potentially disrupt these interactions. Thirteen structurally diverse compounds with favorable *in silico* ADME/Toxicity profiles have been retrieved from this set. Extensive testing of these compounds using cell-based and cell-free systems identified lead compounds that confer considerable protection against PUMA-dependent and radiation-induced apoptosis, and inhibit the interaction between PUMA and Bcl-xL.

**Keywords:** Inhibition of PUMA-induced apoptosis, Bcl-2 protein family, BH3 domain, protein-protein interactions, pharmacophore modeling, druggability, virtual screening of libraries of small compounds.

## INTRODUCTION

Understanding the molecular mechanisms of regulating apoptosis, or programmed cell death, is one of the hottest research areas in biomedical sciences. There is a long list of diseases associated with altered cell survival [1]. Increased apoptosis is characteristic of AIDS, neurodegenerative diseases and various forms of tissue injury. Decreased or inhibited apoptosis is a hallmark of many malignancies and involved in autoimmune disorders and some viral infections. In recent years, enormous efforts have gone into developing modulators of apoptosis for therapeutic purposes. While the damaging effects of ionizing irradiation to cancer cells during clinical radiotherapy involve multiple cell death pathways, the toxicity to normal tissues is mediated primarily by apoptosis. A drug that could ameliorate irradiation induced apoptosis would potentially be of value as a radiation protector and mitigator for use in both clinical radiotherapy and in the setting of treating victims of environmental radiation accidents or radiation terrorism.

Apoptosis occurs via two major signaling pathways in mammalian cells, the *intrinsic* and *extrinsic pathways* [2, 3]. The extrinsic pathway is activated when a pro-apoptotic ligand binds to its receptor that in turn recruits additional proteins to form death-inducing signaling complexes. This

pathway is more extensively utilized by the immune cells. The intrinsic pathway is triggered in diverse cell types by a wide range of stimuli such as developmental cues and severe cellular stress, including DNA damage, deprivation of survival factors nutrients, or loss of cell-cell or cell-matrix attachment, and is mediated through the organelle mitochondrion. Apoptosis is ultimately executed by intracellular protease enzymes called caspases which, upon activation, destroy cellular proteins that are vital for cell survival [4]. The mitochondrial apoptotic pathway is regulated by the evolutionarily conserved Bcl-2 protein family, which includes both pro-apoptotic members such as Bax, Bak that promote mitochondrial permeability, and anti-apoptotic (cell survival) members such as Bcl-2, Bcl-xL, A1 and Mcl-1, which inhibit the mitochondrial release of cytochrome *c* [5, 6]. These two groups share three or four of the characteristic domains of homology (Bcl-2 Homology or BH domains BH1-BH4, composed each of a functional helix). In addition, the Bcl-2 family includes a third group such as Bim, Bad and PUMA, which contain a single BH3 domain, therefore termed "BH3-only proteins". BH3-only proteins are apical sensors of different apoptotic stimuli and function to inhibit Bcl-2 like proteins and/or to activate Bax or Bak [7, 8].

PUMA, p53-Uprelugated Mediator of Appoptosis was initially identified as a transcriptional target of p53 and a mediator of DNA damage-induced apoptosis [9, 10]. PUMA is transcriptionally activated by a wide range of apoptotic stimuli and transduces these proximal death signals to the mitochondria Fig. (1)[11]. PUMA directly binds to all five known anti-apoptotic Bcl-2 family members with high affinities through its BH3 domain. Binding of PUMA to the Bcl-2 like proteins results in the displacement of Bax/Bak

\*Address correspondence to these authors at the University of Pittsburgh School of Medicine, Departments of Computational & Systems Biology and Pathology, Hillman Cancer Center Research Pavilion, 5117 Centre Ave, Pittsburgh, PA, 15213, USA; Tel: 412 648 3332; Fax: 412 648 3163; E-mail: bahar@pitt.edu; Tel: 412 623 7786; Fax: 412 623 7778; E-mail: yuj2@upmc.edu  
# equal contribution

and their activation via formation of multimeric pore like structures on the mitochondrial outer membrane, leading to mitochondrial dysfunction and caspase activation Fig. (1). PUMA is implicated in many pathological and physiological processes including cancer, tissue injury, neurodegenerative diseases, immune response and bacterial or viral infection [11]. Recent work in mice indicates that PUMA is the primary, if not the sole, mediator of p53-dependent radiation-induced apoptosis in the rapidly dividing tissues of the gastrointestinal (GI) tract and hematopoietic (HP) system, and amongst cellular targets including cells and progenitors in the intestinal and hematopoietic systems. Genetic ablation or inhibition of PUMA provides drastic radioprotection in mice [12-15].

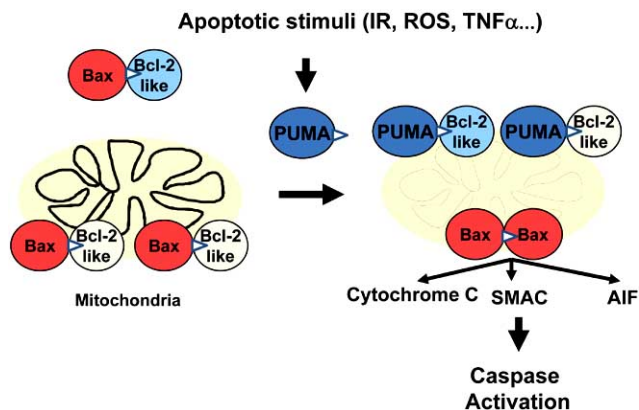


**Fig. (1).** PUMA-mediated apoptosis. PUMA is induced by a wide range of death stimuli, such as gamma-radiation, reactive oxygen species (ROS) and inflammatory cytokines. Binding to the Bcl-2 like proteins by PUMA through its BH3 domain (triangle) leads to activation of Bax/Bak at the mitochondrial membrane, permeabilization of mitochondrial outer membrane, and release of apoptogenic proteins such as cytochrome C, SMAC and AIF. The apoptotic proteins promote activation of caspases and nucleases leading to irreversible cell demise.

The 3D structures of PUMA BH3 domain in complex with anti-apoptotic Bcl-2 proteins Mcl-1 [16] and A1 [17] have been recently determined Fig. (2A). Based on binding properties of BH3-only proteins with Bcl-2 like proteins, Bcl-2 inhibitors have been developed to mimic the actions of the proapoptotic BH3 domains [18, 19]. Considering the importance of the interactions of PUMA/Bcl-2 like proteins in initiating the intrinsic pathway, we describe herein the identification of small molecules that disrupt or prevent these key interactions and consequently suppress the apoptotic response induced by PUMA and gamma irradiation.

## RESULTS

### Sequence and Structure Analysis

Among the Bcl-2 pro-survival proteins, A1 is the most similar to Mcl-1 in terms of binding profile, sharing 25.4% identity and 46.2% similarity over their helical bundles [16]. Fig. (2) displays the shared mechanism of interaction between PUMA BH3 domain (an  $\alpha$ -helix of 22 residues) and these two family members. A 13-residue motif defines the BH binding domain, designated as  $\phi_1\Sigma\text{XX}\phi_2\text{XX}\phi_3\Sigma\text{D}\phi_4\text{L}$ ,

where  $\phi_1$ - $\phi_4$  are hydrophobic residues,  $\Sigma$  designates a small residue, Z is usually an acidic residue, L and D are conserved leucine and aspartate.

As shown in Fig. (2), the sequence and structure alignments of PUMA against the pro-survival proteins A1 and Mcl-1 reveal conserved interactions between three pairs of residues, all found in the BH3 domain: a hydrophobic interaction of PUMA Leu141 with Mcl-1 Phe251 (or A1 Phe95); and two salt bridge interactions between PUMA Arg142 and Mcl-1 Asp237 (or A1 Asp81) and between PUMA Asp146 and Mcl-1 Arg244 (or A1 Arg88).

Note that Mcl-1 and A1 have a root-mean-square deviation (RMSD) of 1.6 Å in their backbone atoms and are most similar in their binding profiles [17]. Upon superimposing the PUMA BH3 domain in complex with Mcl-1 (PDB file 2roc [16] with the PUMA BH3 domain in complex with A1 (PDB file 2vof [17]), this high degree of homology, as well as the three conserved interactions of PUMA are clearly seen Fig. (2). These key interacting residues highlighted in Fig. (2) form the basis of pharmacophore model described below, which we designed for potential inhibitors/mitigators of PUMA activity.

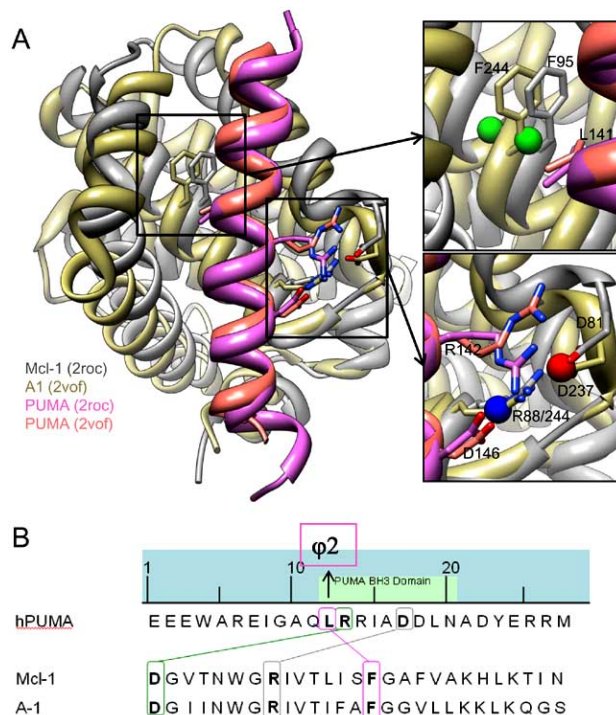


**Fig. (2).** Interactions between PUMA BH3 domain and pro-apoptotic proteins A1 and Mcl-1. (A) Overlay of PUMA bound structures of A1 (PDB code: 2vof [17]) and Mcl-1 (PDB code: 2roc [16]) are shown. Panels show a closer view of key interactions between PUMA and A1/Mcl-1 proteins and the locations of pharmacophore features. The radius of the feature spheres are set to 0.75 Å ( $\frac{1}{4}$  of the actual size in the pharmacophore model) for display purposes. (B) Sequence properties considered in designing the pharmacophore model. Key conserved interactions by sequence alignment include a Leu-Phe hydrophobic interaction (PUMA Leu141.C<sub>δ1</sub> with Mcl-1 Phe251.C<sub>β</sub>, in blue), an Arg-Asp salt-bridge interaction (PUMA Arg142.NH<sub>1</sub> with Mcl-1 Asp237.O<sub>δ2</sub>, in red), and an Asp-Arg salt-bridge interaction (PUMA Asp146.O<sub>δ1</sub> with Mcl-1 Arg244.N<sub>ε</sub> and A-1 Arg88.N<sub>ε</sub>, in green).

## Pharmacophore Development, Database Screening and Generation of Hits

We designed a pharmacophore model Fig. (3) on the basis of the PUMA BH3 domain structure and its interactions in the complexes with A1 and Mcl-1, consistent with previous biochemical measurements. Therefore our pharmacophore model comprises three residues, two of which are engaged in salt bridges with PUMA BH3 domain residues, and the third making hydrophobic contacts, in accord with the conserved Asp Arg, and Phe of Mcl-1 and A1, which play a key role in stabilizing the interactions with PUMA. The 3-dimensional arrangement of these residues has been deduced from the known geometry of the interfacial interactions illustrated in Fig. (2). Quantitative verification of the three conserved interactions was conducted with the Fast Contact 2.0 server [20]. This server estimates the contribution of different pairs of interfacial residues to the overall binding free energy, which confirmed that the ionic Asp-Arg, Arg-Asp and hydrophobic Phe-Leu interactions between the BH3 domain of PUMA and the Mcl-1 or A1 residues make significant contribution to the total binding energy.

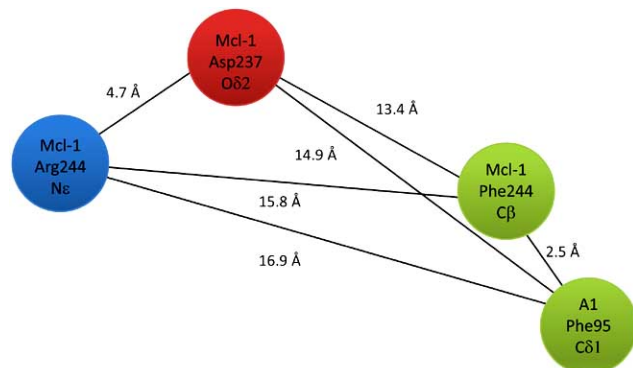


**Fig. (3).** Ligand-based pharmacophore model. Two-dimensional representation of pharmacophore features, with inter-residue distances. Key conserved interactions derived from sequence and structural data include an Asp-Arg salt-bridge interaction (PUMA Asp146.O<sub>δ1</sub> with Mcl-1 Arg244.N<sub>ε</sub> and A-1 Arg88.N<sub>ε</sub>, blue feature), an Arg-Asp salt-bridge interaction (PUMA Arg142.NH<sub>1</sub> with Mcl-1 Asp237.O<sub>δ2</sub>, red feature), and a Leu-Phe hydrophobic interaction (PUMA Leu141.C<sub>δ1</sub> with Mcl-1 Phe251.C<sub>β</sub> and A1 Phe95.C<sub>δ1</sub>, green features).

The resulting PUMA inhibitor pharmacophore model was used to screen the ZINC 8.0 database [21] for lead-like molecules (about  $2.0 \times 10^6$  of them) and extract those sufficiently similar to the pharmacophore model. Up to 250 conformations were generated for each lead-like molecule using MOE2008.10 [22]. The high throughput screening of this large set of compounds against the pharmacophore model captured 142 hits, which were subjected to further examination by both computations and experiments.

### ADME/Tox *in silico* Predictive Analyses

Most failures in clinical trials result from ADME/Tox deficiencies. To mitigate this risk, state-of-the-art drug discovery strategies and programs now incorporate the evalua-

tion and optimization of ADME/Tox properties early in the discovery process. An ADME/Tox filtering might be considered premature at the hit finding stage, however, we applied the *in silico* assessment of ADME/Tox properties to prioritize the 142 compounds that resulted from the initial database screening process, with the understanding that those compounds could potentially serve as drugs. The first round of experiments were therefore performed on compounds that were predicted to have no ADME/Tox liabilities.

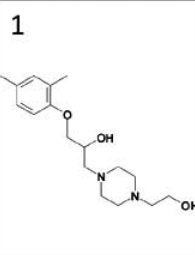
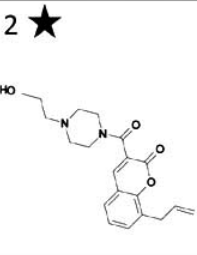
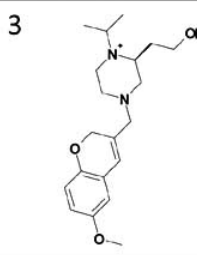
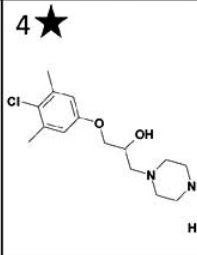
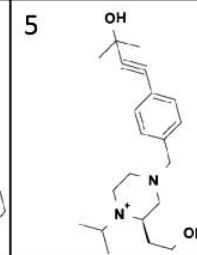
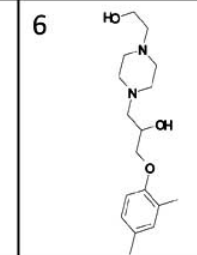
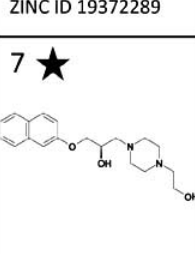
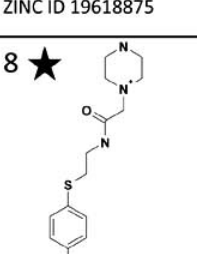
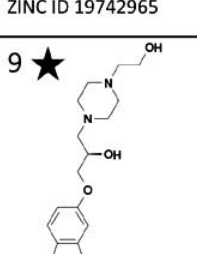
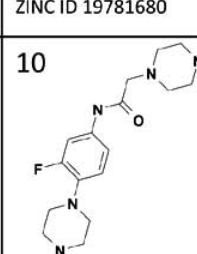
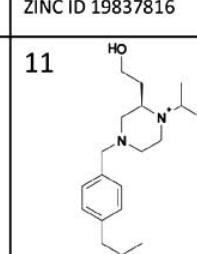
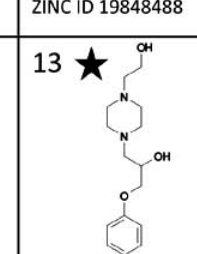
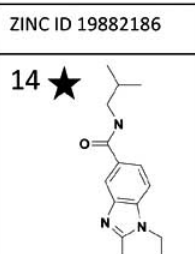
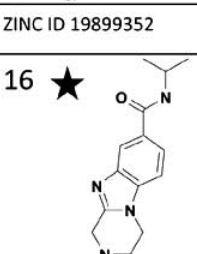
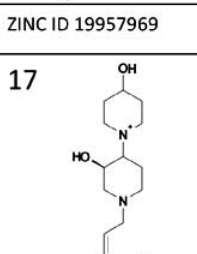
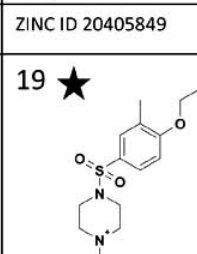
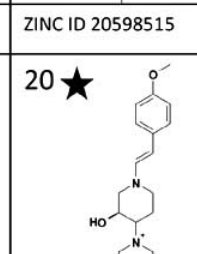
The ACD ADME/TOX software [23, 24] was used to rationally deconvolute the set of hits to extract a set of twenty compounds that passed all the ADME/Tox filters. These compounds selected as potential lead compounds are presented in Fig. (4).

### Druggability Calculations

Protein-protein interfaces are challenging targets. Methods for assessing the druggability of proteins are usually trained using proteins with well-defined active site pockets, and hence are not applicable to protein-protein interfaces in general. Recently, Seco and Barril introduced a first principles-based method that utilizes molecular dynamics (MD) simulations of a binary solvent mixture to identify binding sites and assess their druggability [25]. The binary solvent was composed of 20% isopropanol and 80% water by volume. The choice of isopropanol as the probe molecule is to capture polar-neutral and hydrophobic features of drug-like molecules. The method identifies regions enriched with isopropanol molecules, hot spots, on the protein surface. These hot spots are then used to estimate maximal binding affinity that a drug-like molecule can attain by binding the corresponding site. We performed 16 ns long MD simulations for PUMA, using the structure resolved by Smits *et al.* [17]. We examined where, if any, binding hot spots are located on the PUMA binding surface.

We observed that regions highly concentrated with isopropanol fall on the binding surface of PUMA BH3 domain. The overlay of isopropanol enrichment areas (colored cyan) and the prosurvival protein A1 (light yellow ribbon diagram) is shown in Fig. (5A). Notably, druggability calculations based on BH3 structure only correctly identify the interface with protein A1 to be a highly druggable site. This observation further supports the view that this particular surface region is a promising site for small molecule binding and thereby block PUMA binding to prosurvival proteins.

As a further analysis, we selected six hot spots (cyan) deduced from druggability computations, and calculated the maximal affinity to be 3  $\mu$ M at the region spanned by these hot spots. Selected hotspots and their location with respect to the pharmacophores model sites (blue, red and green spheres) are shown in Fig. (5B). The predicted maximal affinity is considerably low, yet still in the range where MD-based method is able to make reliable predictions [25]. It should also be noted that this method is well suited for estimating the contributions of polar/neutral and hydrophobic groups to binding affinity, and estimates a lower bound in the absence of electrostatic (ionic) interactions. Ideally, a PUMA inhibitor can make favorable charged interactions with the arginine and aspartic acid on PUMA by positioning suitable atoms at the acceptor and donor sites of our pharma-

1 	2 ★ 	3 	4 ★ 	5 	6 
ZINC ID 19372289	ZINC ID 19618875	ZINC ID 19742965	ZINC ID 19781680	ZINC ID 19837816	ZINC ID 19848488
7 ★ 	8 ★ 	9 ★ 	10 	11 	13 ★ 
ZINC ID 19882186	ZINC ID 19899352	ZINC ID 19957969	ZINC ID 20405849	ZINC ID 20598515	ZINC ID 20707440
14 ★ 	16 ★ 	17 	19 ★ 	20 ★ 	
ZINC ID 20719463	ZINC ID 20732753	ZINC ID 20782902	ZINC ID 12909935	ZINC ID 23338424	

**Fig. (4).** Chemical structures of 20 hits from ZINC 8.0 DB screening using the pharmacophore model and ADME/T calculations. 20 structurally diverse hits were extracted by ADME/T calculations, out of 142 identified from the ZINC 8.0 screening against the pharmacophore model. Compounds acquired for experimental testing are marked with a black star. Structures of hit 12, 15 and 18 are not depicted due to intellectual property protection.

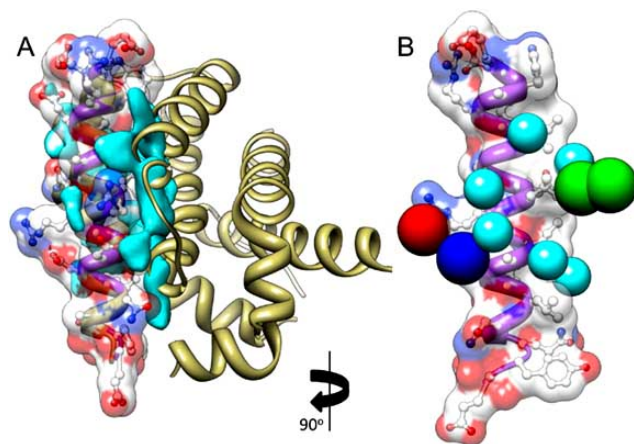


**Fig. (5).** Druggability calculations for PUMA BH3 domain. (A) Regions enriched by isopropanol are shown by the cyan cloud around PUMA. The displayed volume corresponds to enrichment in isopropanol concentration by 4 or more folds over expected concentration. The highly enriched regions correspond to the interface between PUMA and interacting proteins. (B) Isopropanol binding hotspots are shown along with the pharmacophore features. Six hotspots were used to calculate a binding affinity of 3  $\mu$ M, in the absence of ionic interactions.

cophore. Such favorable interactions are not accounted for by the isopropanol probe [25]. Hence, we presume that binding affinities better than 3  $\mu$ M are achievable by targeting the close neighborhood of the selected hotspots with specific pharmacophores.

#### Selected Compounds Inhibited PUMA-Induced Apoptosis

We obtained 13 structurally diverse molecules identified above, or candidate PUMA inhibitors, from commercial sources for testing marked with asterisks in Fig. (4). Various cell-based and cell free systems were used to determine whether these computationally identified PUMA inhibitor had desired biological and biochemical activities. We have previously shown that PUMA induces apoptosis through a Bax and mitochondria-dependent manner in the intestinal epithelium and colon cancer cells [9, 13, 26, 27]. We first analyzed their effects on apoptosis induced by PUMA in DLD1 cells using an adenovirus expressing PUMA [27, 28]. When added at 25  $\mu$ M, ten out of 13 compounds significantly suppressed PUMA-induced apoptosis Fig. (6A). The apoptosis induced by PUMA is completely dependent on its BH3 domain, as the BH3 domain deleted PUMA (Ad- $\Delta$ BH3) was unable to induce apoptosis in DLD1 cells and

several other cell lines Fig. (6A) [28]. In addition, 8 out of 13 compounds significantly inhibited growth suppression induced by PUMA Fig. (6B). Most (11 out of 13) compounds had little or measurable negative effects on proliferation or apoptosis on their own compared with vehicle at doses of 1, 5, 25 and 50  $\mu\text{M}$  Fig. (6C) and data not shown. These results suggest that several compounds identified using the pharmacophore model, are potential PUMA inhibitors.

### Selected Compounds Inhibited PUMA-Dependent and Radiation-Induced Apoptosis

We previously reported that radiation or DNA damaging agent Adriamycin induces apoptosis in HCT116 cells deficient in the cyclin-dependent kinase (CDK) inhibitor p21 (*p21*-KO cells) [27, 29, 30]. Radiation-induced apoptosis is *PUMA*-dependent in *p21*-KO cells, as deleting *PUMA* in these cells (double knockout (*p21*/*PUMA* DKO) significantly blocked radiation-induced apoptosis Fig. (7A). We selected three compounds that significantly suppressed *PUMA*-induced apoptosis and growth suppression (Hits 12, 15 and 18) and examined their effects on radiation-induced apoptosis in this system. When added at 25  $\mu\text{M}$  and 15 min-

utes after irradiation, all three compounds displayed anti-apoptotic activities in *p21* KO cells Fig. (7A). These compounds alone had little or no effects on the proliferation or apoptosis of either cell line at 25 or 50  $\mu\text{M}$  Fig. (7A) and data not shown. We further examined the ability of these three compounds on radiation-induced apoptosis in a relatively radiosensitive germ cell line NCCIT as a stem cell model. When added at 25  $\mu\text{M}$  and 15 minutes after irradiation, all three compounds displayed significant antiapoptotic activities Fig. (7B).

We further evaluated the effects of hit 18 on radiosensitivity of murine hematopoietic cell line 32D cl3. Hit 18 was found to significantly suppress radiosensitivity when added either one hour before or after radiation in a clonogenic assay in doses from 0-6 Gy, reflected by an increase in  $D_{010}$  (final slope of irradiation survival curve expressed in Gy) and  $N$  (shoulder on the survival curve) Fig. (7C). These results suggest that selected compounds were able to inhibit *PUMA*-dependent and radiation-induced apoptosis. Interestingly, hit 18 consistently showed the highest level of protection against both *PUMA*- or radiation-induced apoptosis Figs. (6 and 7).

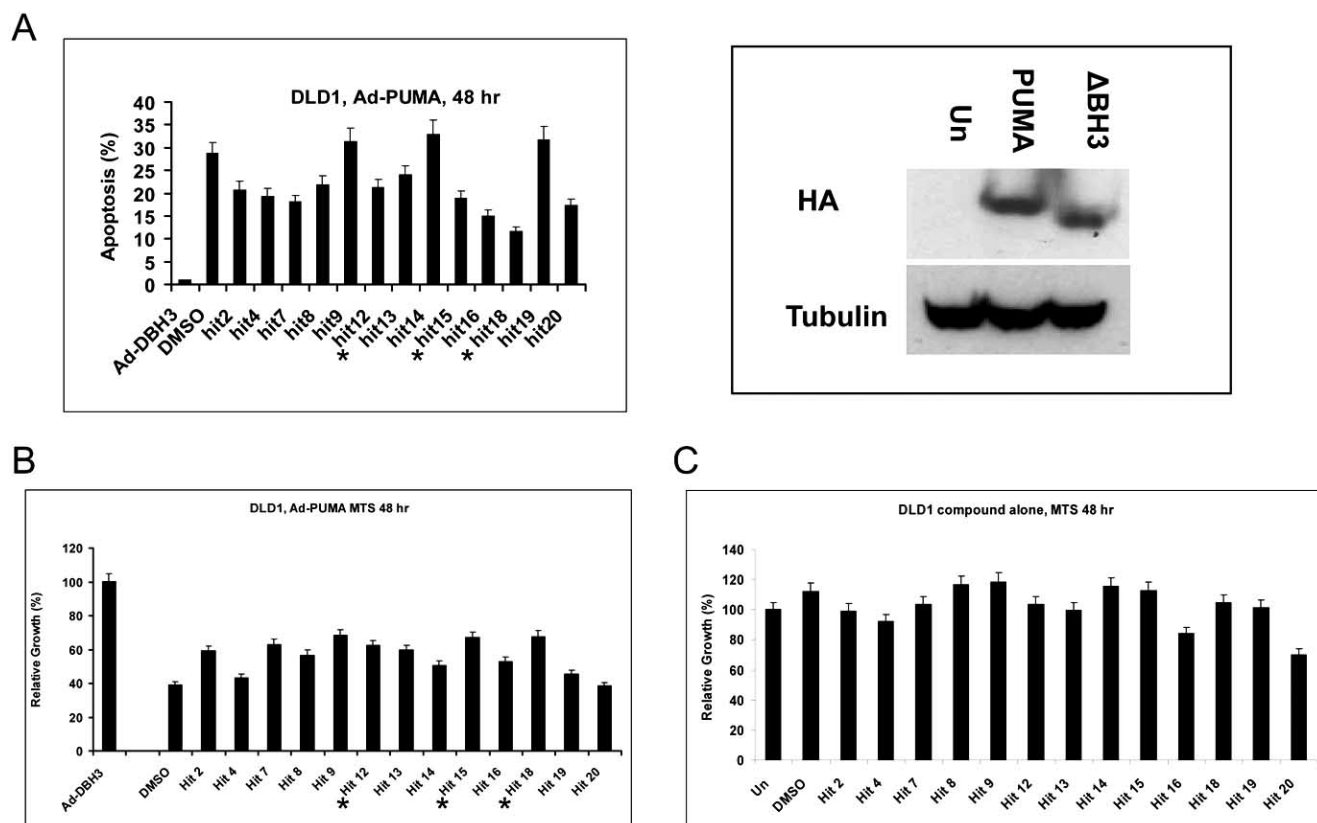


**Fig. (6).** Selected compounds inhibited PUMA-induced apoptosis and growth suppression. DLD1 cells were infected with 10 MOI of Ad-PUMA, or a control Ad- $\Delta\text{BH3}$  with or without the addition of compounds. The compounds were used at 25  $\mu\text{M}$  and added the same time as Ad-PUMA. The cells were analyzed at 48 hr after treatment. (A) The effects of indicated compounds on Ad-PUMA-induced apoptosis were analyzed by nuclear fragmentation assay at 48 hr. Right, the expression of PUMA and the BH3 deleted PUMA ( $\Delta\text{BH3}$ ) was confirmed by Western blotting. Tubulin was used as loading control. \*The P values of hits 12, 15 and 18 vs. DMSO are  $1.3 \times 10^{-3}$ ,  $1.0 \times 10^{-5}$ , and  $1.3 \times 10^{-6}$ , respectively. (B) The cell growth of DLD1 cells was analyzed by MTS assays. \*The P values of hits 12, 15 and 18 vs. DMSO are  $1.2 \times 10^{-7}$ ,  $4.0 \times 10^{-7}$  and  $1.2 \times 10^{-8}$ , respectively. (C) The cell growth of DLD1 cells without Ad-PUMA infection was analyzed by MTS assays. The results are average  $\pm$  SD of three independent experiments, and expressed as values relative to vehicle control.

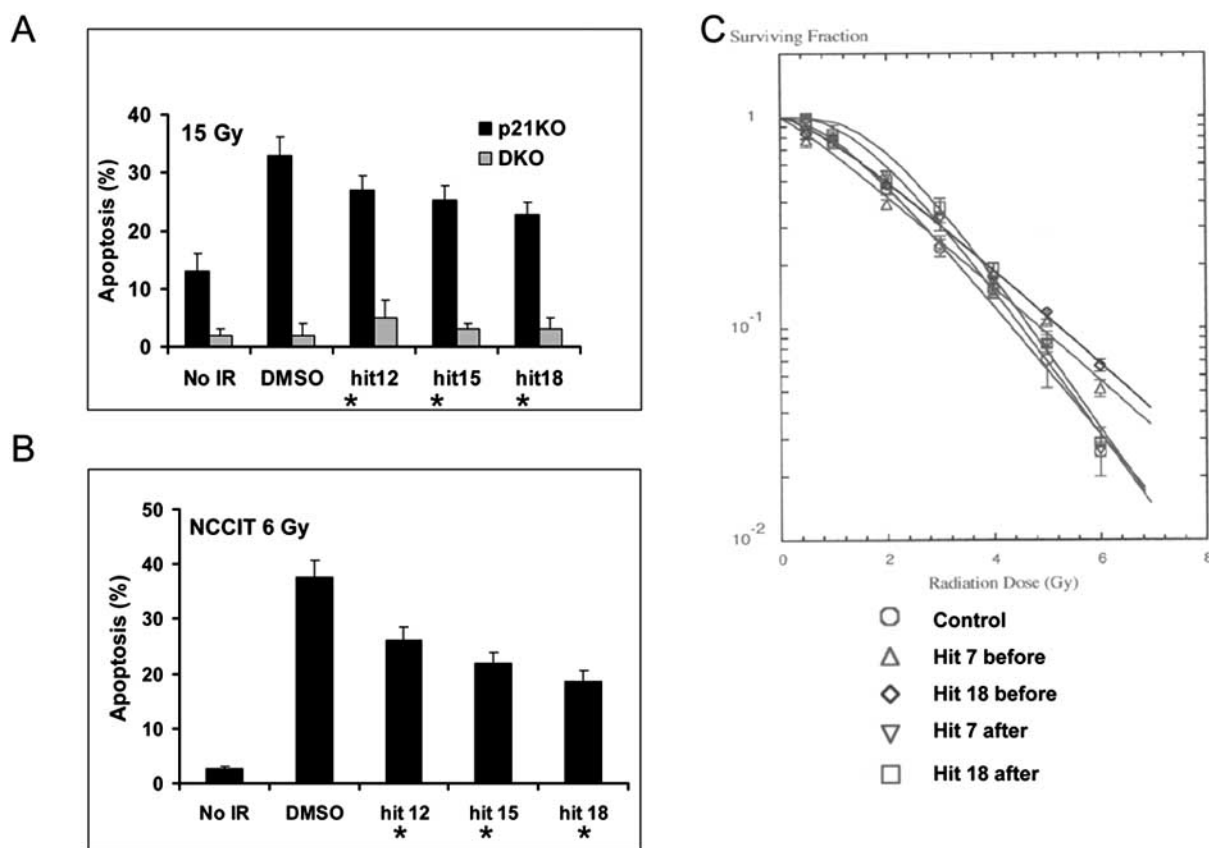


**Fig. (7).** Selected compounds inhibited PUMA-dependent and radiation-induced apoptosis. **(A)** The indicated compounds were added to *p21* KO or *p21/PUMA* DKO cells 15 minutes after irradiation (15 Gy), and apoptosis was scored at 48 hr post-IR. \*The P values of hits 12, 15 and 18 vs. DMSO in *p21* KO cells are  $3.28 \times 10^{-6}$ ,  $7.53 \times 10^{-6}$  and  $4.2 \times 10^{-5}$ , respectively. **(B)** The indicated compounds were added to NCCIT cells 15 minutes after radiation (6 Gy), and apoptosis was scored at 48 hr post-IR. \*The P values of hits 12, 15 and 18 vs. DMSO are  $6.1 \times 10^{-5}$ ,  $2.1 \times 10^{-6}$  and  $6.1 \times 10^{-7}$ , respectively. **(C)** Clonogenic survival of 32D Cl3 cells with two compounds (10  $\mu$ M) added 1 hr before and after IR. Cells were plated and scored as described in the Materials and Methods. Results are the mean  $\pm$  SD of each agent at each concentration.

### Selected Compounds Inhibited the Interaction Between PUMA and Bcl-xL

The BH3 domain of PUMA is capable of binding to all five known antiapoptotic Bcl-2 family members including Bcl-2, Bcl-xL, Mcl-1, Bcl-w and A1 with high affinity, while that from most other BH3-only proteins do so selectively [31, 32]. Prior work suggests that Bcl-xL is a major antiapoptotic Bcl-2 member in human intestinal epithelium [33, 34]. We therefore determined whether these three compounds with promising cellular activities are able to disrupt the interactions between PUMA and Bcl-xL using a cell free system established earlier [34]. In this system, PUMA and Bcl-xL are expressed separately in *BAX* KO HCT 116 cells first to avoid activation of caspases and degradation of cellular proteins, and mixed. HA-tagged PUMA and V5-tagged Bcl-xL interacted strongly by immunoprecipitation in a BH3 domain-dependent fashion Fig. (8A). This interaction is significantly inhibited by two of three compounds Fig. (8B). We also did similar experiments using lysates prepared from 293 cells, which contains BAX protein. Similar results were obtained. Interestingly, hit 18 displayed the strongest effect on disrupting this interaction, correlated with its strongest antiapoptotic effects in cells Figs. (6 and 7).

### DISCUSSION

Mitochondrial damage represents the "point of no return" in the apoptotic pathway, and is highly regulated by a cascade involving mitochondrial membrane permeability, cytochrome *c* leakage, caspase activation and cell demise [7, 35, 36]. The Bcl-2 protein family has been identified as the gateway to mitochondria-mediated apoptosis [37]. The BH3-only protein PUMA integrates diverse death signals through both p53-dependent and -independent mechanisms to initiate apoptosis. Unlike most BH3-only proteins, PUMA neutralizes all five known anti-apoptotic Bcl-2 members through high-affinity interactions, which makes the PUMA BH3 domain an enticing target for drug design.

In the present study, using structural data on the conserved interactions of PUMA with Bcl-2-like proteins Mcl-1 and A1, we developed a pharmacophore model for a potential inhibitor of the interaction of PUMA with Bcl-2 family members. Although targeting protein-protein interactions using small molecules can be difficult, inhibitors may be developed provided that the binding surface of the target protein has druggable features. The deep hydrophobic groove on the surface of Bcl-xL for example proved it feasible to develop highly specific inhibitors of Bcl<sub>xL</sub>-Bad inter-

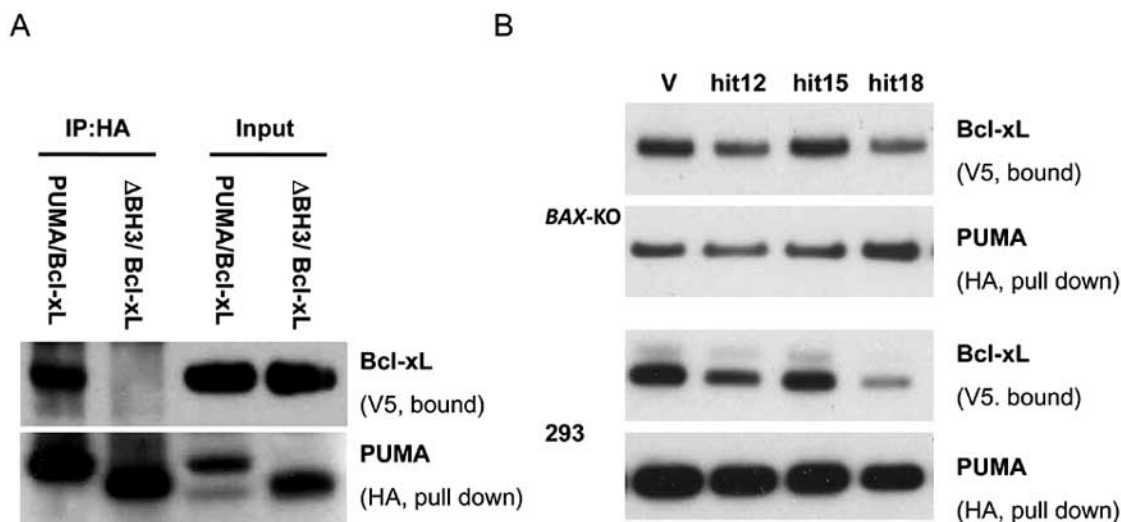


**Fig. (8).** Selected compounds inhibited the interaction between PUMA and Bcl-xL. **(A)** The interaction of PUMA and Bcl-xL in BAX-KO extracts were analyzed by IP. Antibodies against HA were used to pull down PUMA. Western blotting (IB) was performed to analyze Bcl-xL bound to PUMA (V5) and the efficiency for PUMA pull down (HA). Input represents 50% of the starting lysates used for IP. **(B)** The effects of the indicated compounds on the interactions between PUMA and Bcl-xL were analyzed as in **(A)**. Compounds were used at 100  $\mu$ M and 25  $\mu$ M in BAX-KO and 293 lysates, respectively. The vehicle (DMSO, V) or compounds were incubated with PUMA lysates for 15 minutes prior to the addition of V5-Bcl-xL lysates.

action [38]. The pharmacophore model developed here is based on the amino acid identities and geometry of specific recognition residues on two proteins that bind PUMA. *In silico* screening of the ZINC 8.0 database, and *in silico* ADME/Toxicity profiles, complemented by druggability calculations in support of the adopted strategy, led to a small set of lead compounds that are further screened and validated using assays. The working concentrations of several compounds in cells are between 10-25  $\mu$ M, not too far from the predicted 3  $\mu$ M.

PUMA inhibitors can have several applications. Given a prominent role of PUMA in DNA damage induced apoptosis in the GI tract [13, 39] and HP systems [14, 15], PUMA inhibitors are expected to provide radiation protection and mitigation. PUMA transcription induction occurs within 8 hr following radiation while protein levels remain elevated beyond 24 hours. Inhibiting PUMA binding to Bcl-2 like proteins is likely to provide a wider window for intervention, compared to inhibiting its transcription, a critical consideration of mitigation measures administered after a radiation accident or attack. PUMA inhibitors might also prevent or mitigate intestinal damage and apoptosis induced by inflammatory cytokines, reactive oxygen species or chemotherapy [40, 41] Fig. (1), some of which are implicated in the delayed phase of radiation damage [42, 43]. Furthermore, it should not be surprising and perhaps even desirable that PUMA inhibitors identified in this study can function as Pan-BH3 inhibitors based on several highly conserved interactions of the BH3 domain with Bcl-2 like proteins [16, 17]. Since p53 ablation leads to high risks in cancer [44] and exacerbated IR-induced GI damage [45], inhibiting PUMA might be more advantageous compared to p53 in tissue protection. Additional work and optimization of the lead structures identified in this study can guide their further development.

Apoptosis evasion is a hall mark of cancer [46]. Resistance to apoptosis is commonly associated with altered expression in both pro- and anti-apoptotic Bcl-2 family members, and contributes to tumor formation, progression and impaired responsiveness to anticancer therapies [11, 3, 47]. Expression of PUMA rapidly kills a variety of human cancer cells, and results in profound chemo- or radio-sensitization and [11, 27, 48]. Therefore, an analogous strategy can be used to develop PUMA mimetics as Pan-Bcl-2 inhibitors. In fact, this possibility has been explored and led to the development of a selective Bcl-2 and Bcl-xL inhibitor ABT-737 and analogs, currently in clinical trials [18, 19]. Interestingly, resistance to ABT-737 is attributable to Mcl-1 overexpression in some cases [49], where Pan-Bcl-2 inhibitors might be useful.

In summary, the interaction of PUMA/Bcl-2 like proteins is a critical regulatory step in apoptosis initiation. The structural features of this interactions and its dependence on a rather small PUMA BH3 domain make it an attractive target for drug development. PUMA inhibitors might be effective and safe in radiation protection and mitigation and perhaps in other types of tissue injury associated with apoptosis.

## METHODS

### Ligand-Based Pharmacophore Modeling

Ligand-based development of a pharmacophore model uses the spatial information of known ligands (or binding proteins) for topological description of ligand-receptor interactions and for the subsequent discovery of new structural leads. In this study, pharmacophore features that complement the BH3 domain were built upon both sequence analysis of hPUMA and structural analysis of the BH3 domain of PUMA in complex with Mcl-1 (PDB entry 2roc) [16] and A1 (PDB entry 2vof) [17]. The pharmacophore model was

built by applying the PGH (Polarity-Charged-Hydrophobicity) scheme in MOE 8.0 software [22].

### Database (DB) Searching

The ZINC 8.0 DB [21] containing approximately  $2.0 \times 10^6$  lead-like compounds was used for screening. Compared to *de novo* design methods, known DB searching offers the advantage that hits can be purchased for testing. For each compound in the DB, alternative conformations were generated allowing for a maximum conformational energy of 20 kcal/mol above the lowest-energy found. The number of conformers generated for each compound was limited to a maximum number of 250.

### ADME/Toxicity Predictions

Computational modeling tools were used to estimate the bioavailability, aqueous solubility, blood brain barrier potential, human intestinal absorption, the cytochrome P450 (*i.e.* CYP2D6) enzyme inhibition potential, mutagenicity, and hERG inhibition of the hits obtained from the database screening. The bioavailability, aqueous solubility, and human intestinal absorption were estimated using the ACD/ADME Boxes software (ACD Labs, Toronto, Canada) [23, 24], while mutagenicity, hERG and CYP2D6 inhibition were estimated with ACD/TOX screening (ACD Labs, Toronto, Canada) [23, 24].

### Druggability Index Calculations

We applied druggability index calculations introduced by Seco *et al.* [25]. In our work, we used NAMD [50] program and CHARMM force field [51]. To prevent protein rotation and translation, we applied 0.01 kcal/mol harmonic restraints on  $\alpha$ -carbons. Threonine side-chain atom types and partial charge set used by Seco and Barril was used to define isopropanol topology in CHARMM format [51]. Hotspot identification and druggability index calculations were performed using the procedure described by Seco *et al.* [25].

### Cell Culture and Treatment

All cell lines were maintained at 37°C and with 5% CO<sub>2</sub>. Colon cancer cell lines DLD1 and HCT116 derivative lines (BAX KO-knock-out cells [33], *p21* KO – *p21* knock-out cells [52], PUMA and *p21* KO cells [27]) were cultured in McCoy's 5A media (Invitrogen). The germ cell tumor line NCCIT and kidney epithelial cell line 293 were obtained from ATCC and cultured with RPMI-1640 medium (Mediatech) and DMEM (Invitrogen), respectively. The IL-3 dependent murine hematopoietic progenitor cell line 32D c1 3 was grown in McCoys modified medium [53, 54]. All cell culture media were supplemented with 10% defined fetal bovine serum (Hyclone), 100 units/ml penicillin, and 100 µg/ml streptomycin (Invitrogen).

Cells were plated in 12-well plates at ~20% density and allowed to attach for 12-16 hr prior to adenovirus infection or irradiation. The DLD1 cells were infected with 0.01 µl of virus, an equivalent 10 multiplicity of infection (MOI) [28]. The constructions and purification of recombinant adenoviruses, Ad-PUMA and Ad- $\Delta$ BH3 were previously described [27, 48]. Cells were irradiated at dose rate 100 cGy/min

ranging from 6 to 15 Gy using a <sup>137</sup>Cs irradiator (Mark I, JL Shepherd and Associates, San Fernando, CA, USA). PUMA inhibitors (25 µM or as indicated) were added to the media following irradiation. Thirteen small molecules with defined structures were purchased from either InterBioScreen (Russia) or Chembridge (San Diego, CA, USA) and details are available upon request. The three compounds used in the validation were hits 12, 15 and 18.

### Analysis of Apoptosis and Cell Growth

Following treatment, floating and adhering cells were collected at 48 hr. For analysis of apoptosis by nuclear staining, cells were resuspended and fixed in PBS solution containing 3.7% formaldehyde, 0.5% Nonidet P-40 and 10 µg/ml Hoechst 33258 (Molecular Probes). Apoptosis was assessed through microscopic visualization of condensed chromatin and micronucleation as previously described [48, 55]. A minimum of 300 cells were analyzed in triplicate. Cell growth was measured by the 3-(4,5-dimethyl-thiazol-2-yl)-5-(3-carboxymethoxyphenyl)-2-(4-sulfophenyl)-2Htetrazolium (MTS) assay in 96-well plates (2,500 cells per well) using CellTiter 96 Aqueous One Solution (Promega) as described [49, 57]. Each experiment was repeated at least twice in triplicate. For irradiation survival curves, 32D cells were irradiated over a total dose range of 0 to 8 Gy. The cells were incubated with compounds 1 hr before or after irradiation at 10 µM. Irradiated cells were centrifuged to a cell pellet and resuspended in medium then plated in 0.8% methylcellulose containing medium for clonogenic survival curve assay. Cells were plated at 500, 1000, or 2000 cells per plate in triplicate at each dose, and the colonies of greater than 50 cells were counted at day 7 according to published methods [53, 54]. Data are processed by software as described [54].

### Antibodies and Western Blotting

The antibodies used for Western blotting include antibodies against HA (Santa Cruz (rabbit)), HA (Roche (mouse)) and anti-V5 antibody (Invitrogen). Western blotting analysis was performed as previously described [28, 56].

### Immunoprecipitation

BAX KO HCT 116 cells or 293 cells were transfected with HA-PUMA and V<sub>5</sub>-Bcl-xL by Lipofectamine<sup>TM</sup> 2000 (Invitrogen) following the instructions of the manufacturer. The expression plasmids of HA tagged PUMA and V<sub>5</sub>-tagged Bcl-xL were previously described [9]. Transfection and immunoprecipitation was performed as described with minor modifications [35]. In brief, twenty-four hrs after transfection, cells in one T-75 flask were harvested and resuspended in 1 ml of EBC buffer (50 mM Tris-HCl, pH 7.5, 100 mM NaCl, 0.5% NP-40) supplemented with protease inhibitor cocktail (Roche Applied Sciences). The cell suspension were disrupted by sonication and then spun at 10,000 × g for 10 min to collect the cell lysates (supernatant). The lysates from HA-PUMA and V<sub>5</sub>-Bcl-xL transfections were mixed and incubated with a compound (100 µM) with gentle rotation for 1 h at RT. Compounds or DMSO were incubated with PUMA extracts 15 minutes before the addition of Bcl-xL extracts. The mixture was then incubated with 50 µl Dynabeads<sup>®</sup> Protein A (Invitrogen)

with antibody bound for 1 hr at RT following the instructions of the manufacturer. For immunoprecipitation (IP), 1  $\mu$ g of IP antibodies (HA) were added to cell lysates diluted with the binding buffer in a total volume of 200  $\mu$ l. Following the final wash in a new tube, the immunocomplexes on the beads were eluted with 50  $\mu$ l of 2  $\times$  Laemmli sample buffer, heated at 95°C for 10 min, and analyzed by Western blotting.

## ACKNOWLEDGEMENT

This work is supported by NIH U19A1068021 (JSG, IB and JY), 1R01GM086238-01 (IB), and UO1DK085570 (JY).

## REFERENCES

- Thompson, C.B. Apoptosis in the pathogenesis and treatment of disease. *Science*, **1995**, *267*(5203), 1456-1462.
- Fulda, S.; Debatin, K.M. Extrinsic versus intrinsic apoptosis pathways in anticancer chemotherapy. *Oncogene*, **2006**, *25*(34), 4798-4811.
- Adams, J.M.; Cory, S. The Bcl-2 apoptotic switch in cancer development and therapy. *Oncogene*, **2007**, *26*(9), 1324-1337.
- Thornberry, N.A.; Lazebnik, Y. Caspases: enemies within. *Science*, **1998**, *281*(5381), 1312-1316.
- Antonsson, B.; Conti, F.; Ciavatta, A.; Montessuit, S.; Lewis, S.; Martinou, I.; Bernasconi, L.; Bernard, A.; Mermod, J.J.; Mazzei, G.; Maundrell, K.; Gambale, F.; Sadoul, R.; Martinou, J.C. Inhibition of Bax channel-forming activity by Bcl-2. *Science*, **1997**, *277*(5324), 370-372.
- Bagci, E.Z.; Vodovotz, Y.; Billiar, T.R.; Ermentrout, G.B.; Bahar, I. Bistability in apoptosis: roles of bax, bcl-2, and mitochondrial permeability transition pores. *Biophysics*, **2006**, *90*(5), 1546-1559.
- Yu, J.; Zhang, L. Apoptosis in human cancer cells. *Curr. Opin. Oncol.*, **2004**, *16*(1), 19-24.
- Puthalakath, H.; Strasser, A. Keeping killers on a tight leash: transcriptional and post-translational control of the pro-apoptotic activity of BH3-only proteins. *Cell Death Differ.*, **2002**, *9*(5), 505-512.
- Yu, J.; Zhang, L.; Hwang, P.M.; Kinzler, K.W.; Vogelstein, B. PUMA induces the rapid apoptosis of colorectal cancer cells. *Mol. Cell*, **2001**, *7*(3), 673-682.
- Nakano, K.; Vousden, K.H. PUMA, a novel proapoptotic gene, is induced by p53. *Mol. Cell*, **2001**, *7*(3), 683-694.
- Yu, J.; Zhang, L. PUMA, a potent killer with or without p53. *Oncogene*, **2008**, *27* (Suppl 1), S71-83.
- Potten, C.S. Radiation, the ideal cytotoxic agent for studying the cell biology of tissues such as the small intestine. *Radiat. Res.*, **2004**, *161*(2), 123-136.
- Qiu, W.; Carson-Walter, E. B.; Liu, H.; Epperly, M.; Greenberger, J. S.; Zambetti, G. P.; Zhang, L.; Yu, J. PUMA regulates intestinal progenitor cell radiosensitivity and gastrointestinal syndrome. *Cell Stem Cell*, **2008**, *2*(6), 576-583.
- Wu, W. S.; Heinrichs, S.; Xu, D.; Garrison, S. P.; Zambetti, G. P.; Adams, J. M.; Look, A. T. Slug antagonizes p53-mediated apoptosis of hematopoietic progenitors by repressing puma. *Cell*, **2005**, *123*(4), 641-653.
- Yu, H.; Shen, H.; Yuan, Y.; Xufeng, R.; Hu, X.; Garrison, S. P.; Zhang, L.; Yu, J.; Zambetti, G.; Cheng, T. Deletion of Puma protects hematopoietic stem cells and confers long-term survival in response to high-dose  $\gamma$ -irradiation. *Blood*, **2010**, *115*(17), 3472-3480.
- Day, C. L.; Smits, C.; Fan, F. C.; Lee, E. F.; Fairlie, W. D.; Hinds, M. G. Structure of the BH3 domains from the p53-inducible BH3-only proteins Noxa and Puma in complex with Mcl-1. *J. Mol. Biol.*, **2008**, *380*(5), 958-971.
- Smits, C.; Czabotar, P.E.; Hinds, M.G.; Day, C.L. Structural plasticity underpins promiscuous binding of the prosurvival protein A1. *Structure*, **2008**, *16*(5), 818-829.
- Oltersdorf, T.; Elmore, S.W.; Shoemaker, A.R.; Armstrong, R.C.; Augeri, D.J.; Belli, B.A.; Bruncko, M.; Deckwerth, T. L.; Dinges, J.; Hajduk, P. J.; Joseph, M. K.; Kitada, S.; Korsmeyer, S. J.; Kunzer, A. R.; Letai, A.; Li, C.; Mittin, M. J.; Nettlesheim, D. G.; Ng, S.; Nimmer, P. M.; O'Connor, J. M.; Oleksijew, A.; Petros, A. M.; Reed, J. C.; Shen, W.; Tahir, S. K.; Thompson, C. B.; Tomaselli, K. J.; Wang, B.; Wendt, M. D.; Zhang, H.; Fesik, S. W.; Rosenberg, S. H. An inhibitor of Bcl-2 family proteins induces regression of solid tumours. *Nature*, **2005**, *435*(7042), 677-681.
- Zhang, L.; Ming, L.; Yu, J. BH3 mimetics to improve cancer therapy: mechanisms and examples. *Drug Resist. Updat*, **2007**, *10*(6), 207-217.
- Camacho, C. J.; Zhang, C. FastContact: rapid estimate of contact and binding free energies. *Bioinformatics*, **2005**, *21*(10), 2534-2536.
- Irwin, J. J.; Shoichet, B. K. ZINC--a free database of commercially available compounds for virtual screening. *J. Chem. Inf. Model.*, **2005**, *45*(1), 177-182.
- Molecular Operating Environment (MOE), <http://www.chemcomp.com>, **2008**.
- Japertas, P.; Didziapetris, R.; Petrauskas, A. Fragmental methods in the analysis of biological activities of diverse compound sets, *Mini. Rev. Med. Chem.*, **2003**, *3*(8), 797-808.
- ACD/Labs, <http://www.acdlabs.com>, **ADME/TOX Boxes**, **2009**.
- Seco, J. Luque, F. J.; Barril, X. Binding site detection and druggability index from first principles. *J. Med. Chem.*, **2009**, *52*(8), 2363-2371.
- Yu, J.; Wang, P.; Ming, L.; Wood, M.A.; Zhang, L. SMAC/Diablo mediates the proapoptotic function of PUMA by regulating PUMA-induced mitochondrial events. *Oncogene*, **2007**, *26*(29), 4189-4198.
- Yu, J.; Wang, Z.; Kinzler, K.W.; Vogelstein, B.; Zhang, L. PUMA mediates the apoptotic response to p53 in colorectal cancer cells. *Proc. Natl. Acad. Sci. USA*, **2003**, *100*(4), 1931-1936.
- Yu, J.; Yue, W.; Wu, B.; Zhang, L. PUMA sensitizes lung cancer cells to chemotherapeutic agents and irradiation. *Clin. Cancer Res.*, **2006**, *12*(9), 2928-2936.
- Waldman, T.; Kinzler, K.W.; Vogelstein, B. p21 Is Necessary For the p53-Mediated G(1) Arrest In Human Cancer Cells. *Cancer Res.*, **1995**, *55*(22), 5187-5190.
- Polyak, K.; Waldman, T.; He, T.-C.; Kinzler, K.W.; Vogelstein, B. Genetic determinants of p53 induced apoptosis and growth arrest. *Genes Devel.*, **1996**, *10*(15), 1945-1952.
- Chen, L.; Willis, S.N.; Wei, A.; Smith, B.J.; Fletcher, J.I.; Hinds, M.G.; Colman, P.M.; Day, C.L.; Adams, J.M.; Huang, D.C. Differential targeting of prosurvival Bcl-2 proteins by their BH3-only ligands allows complementary apoptotic function. *Mol. Cell*, **2005**, *17*(3), 393-403.
- Kuwana, T.; Bouchier-Hayes, L.; Chipuk, J.E.; Bonzon, C.; Sullivan, B.A.; Green, D.R.; Newmeyer, D.D. BH3 domains of BH3-only proteins differentially regulate Bax-mediated mitochondrial membrane permeabilization both directly and indirectly. *Mol. Cell*, **2005**, *17*(4), 525-535.
- Zhang, L.; Yu, J.; Park, B.H.; Kinzler, K.W.; Vogelstein, B. Role of BAX in the apoptotic response to anticancer agents. *Science*, **2000**, *290*(5493), 989-992.
- Ming, L.; Wang, P.; Bank, A.; Yu, J.; Zhang, L. PUMA dissociates Bax and BCL-xL to induce apoptosis in colon cancer cells. *J. Biol. Chem.*, **2006**, *281*(23), 16034-16042.
- Wang, X. The expanding role of mitochondria in apoptosis. *Genes Dev.*, **2001**, *15*(22), 2922-2933.
- Green, D.R.; Reed, J.C. Mitochondria and apoptosis. *Science*, **1998**, *281*(5381), 1309-1312.
- Leibowitz, B.; Yu, J. Mitochondrial signaling in cell death via the Bcl-2 family. *Cancer Biol. Ther.*, **2010**, *9*(6), 417-422.
- Petros, A. M.; Nettlesheim, D. G.; Wang, Y.; Olejniczak, E. T.; Meadows, R. P.; Mack, J.; Swift, K.; Matayoshi, E. D.; Zhang, H.; Thompson, C. B.; Fesik, S. W. Rationale for Bcl-xL/Bad peptide complex formation from structure, mutagenesis, and biophysical studies. *Protein Sci.*, **2000**, *9*(12), 2528-2534.
- Qiu, W.; Leibowitz, B.; Zhang, L.; Yu, J. Growth factors protect intestinal stem cells from radiation-induced apoptosis by suppressing PUMA through the PI3K/AKT/p53 axis. *Oncogene*, **2010**, *29*, 1622-1632.
- Wu, B.; Qiu, W.; Wang, P.; Yu, H.; Cheng, T.; Zambetti, G. P.; Zhang, L.; Yu, J. p53 independent induction of PUMA mediates intestinal apoptosis in response to ischaemia-reperfusion. *Gut*, **2007**, *56*(5), 645-654.
- Wang, P.; Wang, P.; Qiu, W.; Dudgeon, C.; Liu, H.; Huang, C.; Zambetti, G. P.; Yu, J.; Zhang, L. PUMA is directly activated by NF-kappaB and contributes to TNF-alpha-induced apoptosis. *Cell Death Differ.*, **2009**, *16*(9), 1192-1202.

- [42] Mothersill, C.; Seymour, C. B. Radiation-induced bystander effects--implications for cancer. *Nat. Rev. Cancer*, **2004**, *4*(2), 158-164.
- [43] Epperly, M. W.; Travis, E. L.; Sikora, C.; Greenberger, J. S. Manganese [correction of Magnesium] superoxide dismutase (MnSOD) plasmid/liposome pulmonary radioprotective gene therapy: modulation of irradiation-induced mRNA for IL-1, TNF-alpha, and TGF-beta correlates with delay of organizing alveolitis/fibrosis. *Biol. Blood Marrow Trans.*, **1999**, *5*(4), 204-214.
- [44] Donehower, L. A.; Harvey, M.; Slagle, B. L.; McArthur, M. J.; Montgomery, C. A. Jr. Butel, J.S.; Bradley, A. Mice deficient for p53 are developmentally normal but susceptible to spontaneous tumours. *Nature*, **1992**, *356*(6366), 215-221.
- [45] Komarova, E. A.; Kondratov, R. V.; Wang, K.; Christov, K.; Golovkina, T. V.; Goldblum, J. R.; Gudkov, A. V. Dual effect of p53 on radiation sensitivity : p53 promotes hematopoietic injury, but protects from gastro-intestinal syndrome in mice. *Oncogene*, **2004**, *23*(19), 3265-3271.
- [46] Hanahan, D.; Weinberg, R. A. The hallmarks of cancer. *Cell*, **2000**, *100*(1), 57-70.
- [47] Fesik, S.W. Promoting apoptosis as a strategy for cancer drug discovery. *Nat. Rev. Cancer*, **2005**, *5*(11), 876-885.
- [48] Sun, Q.; Sakaida, T.; Yue, W.; Gollin, S. M.; Yu, J. Chemosensitization of head and neck cancer cells by PUMA. *Mol. Cancer Ther.*, **2007**, *6*(12), 3180-3188.
- [49] van Delft, M. F.; Wei, A. H.; Mason, K. D.; Vandenberg, C. J.; Chen, L.; Czabotar, P. E.; Willis, S. N.; Scott, C. L.; Day, C. L.; Cory, S.; Adams, J. M.; Roberts, A. W. The BH3 mimetic ABT-737 targets selective Bcl-2 proteins and efficiently induces apoptosis via Bak/Bax if Mcl-1 is neutralized. *Cancer Cell*, **2006**, *10*(5), 389-399.
- [50] Phillips, J. C.; Braun, R.; Wang, W.; Gumbart, J.; Tajkhorshid, E.; Villa, E.; Chipot, C.; Skeel, R. D.; Kale, L.; Schulten, K. Scalable molecular dynamics with NAMD. *J. Comput. Chem.*, **2005**, *26*(16), 1781-1802.
- [51] Brooks, B. R.; Brooks, C. L<sup>III</sup>; Mackerell, A. D.Jr.; Nilsson, L.; Petrella, R. J.; Roux, B.; Won, Y.; Archontis, G.; Bartels, C.; Boresch, S.; Caffisch, A.; Caves, L.; Cui, Q.; Dinner, A. R.; Feig, M.; Fischer, S.; Gao, J.; Hodoseck, M.; Im, W.; Kuczera, K.; Lazaridis, T.; Ma, J.; Ovchinnikov, V.; Paci, E.; Pastor, R. W.; Post, C. B.; Pu, J. Z.; Schaefer, M.; Tidor, B.; Venable, R. M.; Woodcock, H. L.; Wu, X.; Yang, W.; York, D. M.; Karplus, M. CHARMM: the biomolecular simulation program. *J. Comput. Chem.*, **2009**, *30*(4), 1545-1614.
- [52] Wang, P.; Yu, J.; Zhang, L. The nuclear function of p53 is required for PUMA-mediated apoptosis induced by DNA damage. *Proc. Natl. Acad. Sci. USA*, **2007**, *104*(10), 4054-4059.
- [53] Epperly, M. W.; Osipov, A. N.; Martin, I.; Kawai, K. K.; Borisenko, G. G.; Tyurina, Y. Y.; Jefferson, M.; Bernarding, M.; Greenberger, J.S.; Kagan, V.E. Ascorbate as a "redox sensor" and protector against irradiation-induced oxidative stress in 32D CL 3 hematopoietic cells and subclones overexpressing human manganese superoxide dismutase. *Int. J. Radiat. Oncol. Biol. Phys.*, **2004**, *58*(3), 851-861.
- [54] Epperly, M. W.; Bernarding, M.; Gretton, J.; Jefferson, M.; Nie, S.; Greenberger, J. S. Overexpression of the transgene for manganese superoxide dismutase (MnSOD) in 32D cl 3 cells prevents apoptosis induction by TNF-alpha, IL-3 withdrawal, and ionizing radiation. *Exp. Hematol.*, **2003**, *31*(6), 465-474.
- [55] Yu, J.; Zhang, L.; Hwang, P. M.; Rago, C.; Kinzler, K. W.; Vogelstein, B. Identification and classification of p53-regulated genes. *Proc. Natl. Acad. Sci. USA*, **1999**, *96*(25), 14517-14522.
- [56] Sun, Q.; Ming, L.; Thomas, S. M.; Wang, Y.; Chen, Z. G.; Ferris, R. L.; Grandis, J. R.; Zhang, L.; Yu, J. PUMA mediates EGFR tyrosine kinase inhibitor-induced apoptosis in head and neck cancer cells. *Oncogene*, **2009**, *28*(24), 2348-2357.